

# Study of thermal durability properties of tannin–lignosulfonate adhesives

Lucie Chupin · Bertrand Charrier · Antonio Pizzi · Arturo Perdomo · Fatima Charrier-El Bouhtoury

Received: 25 March 2014 / Accepted: 28 November 2014 / Published online: 24 December 2014  
© Akadémiai Kiadó, Budapest, Hungary 2014

**Abstract** This paper aims to study certain aspects of the preparation of tannin–lignin adhesives. Mimosa tannins and lignosulfonates were used in wood adhesives formulation to substitute resins based on formaldehyde. Two ammonium lignosulfonates and two sodium lignosulfonates were glyoxalated to be more reactive. The thermal stability of the lignosulfonates before and after glyoxalation was analysed by thermogravimetric analysis (TG) and differential scanning calorimetry (DSC). The proportion of mimosa tannins and sodium lignosulfonates varied from 20 % tannins to 60 % tannins. 40 % of mimosa tannins were mixed with either glyoxalated sodium lignosulfonates or glyoxalated ammonium lignosulfonates. The thermal properties of the resins were studied by TG, DSC and thermomechanical analysis (TMA). The results showed that after glyoxalation, the degradation of lignosulfonates started at 125 °C instead of 171 °C for the non-glyoxalated lignosulfonates. The results obtained showed that the 40 mass% tannins resin was the most efficient. The TMA results showed that the curing of the resins started at 100–110 °C. The TG and DSC results of the cured resins showed a thermal stability of the adhesives up to approximately 200 °C.

**Keywords** Mimosa tannin · Lignosulfonate · Tannin–glyoxalated lignin adhesive · Glyoxalation

## Introduction

Most wood adhesives used today are amino resins (urea-formaldehyde, melamine-formaldehyde, etc.), phenol formaldehyde and resorcinol formaldehyde resins [1, 2]. With increasing oil prices and the desire to reduce formaldehyde emissions, natural materials have been used to partially or totally substitute formaldehyde.

Lignin is the second most abundant natural polymer after cellulose. The structure of lignin, with the presence of aliphatic hydroxyl groups and phenolic groups, has made it a good partial replacement of phenol for phenol formaldehyde adhesives [3–9]. In recent years, lignin-pMDI (polymeric isocyanate)-phenolic resins were produced with glyoxalated lignins [10, 11]. The glyoxalation of the lignins was found to be an alternative to premethylation of lignins, which increases the reactivity of lignins [11]. Glyoxal is a non-volatile, non-toxic aldehyde [12]. It has been used to make lignin-based adhesives [11] and tannin–lignin adhesives [13]. Glyoxal has also been used as a hardener for tannin-based adhesives for particle board bonding with good mechanical properties [14]. Fourier transformed infrared spectroscopy (FTIR) has been used in order to understand the reaction of glyoxalation for organosolv and kraft lignins [15, 16].

Tannins from many different plants have been used to make wood adhesives, such as grape pomace [17], chestnut [18], pecan nut [19], mimosa [20, 21], and maritime pine [22]. Until the mid 2000s, tannins were used to substitute phenol in phenol-formaldehyde resins [23–26]. Pichelin [27] showed that hexamine is a hardener with equivalent

L. Chupin (✉) · B. Charrier · F. Charrier-El Bouhtoury  
IUT des Pays de l'Adour, IPREM, UMR 5254 CNRS/UPPA,  
371 Rue du Ruisseau, BP 201, 40004 Mont de Marsan, France  
e-mail: lucie.chupin@univ-pau.fr

A. Pizzi  
ENSTIB-LERMAB, University of Lorraine, 27 rue Philippe  
Seguin, BP 1041, 88051 Épinal, France

A. Perdomo  
Tembec, 1154 avenue du Général Leclerc, 40400 Tartas, France

properties to formaldehyde or paraformaldehyde. Tannin–hexamine-based adhesives have been formulated and presented good mechanical properties that were evaluated with thermomechanical analysis [28, 29].

In recent years, tannin–lignin-based adhesives have been developed. The tannins used were mimosa tannins with either organosolv lignins or kraft lignins [13, 21, 30]. FTIR has been used to characterise resins since it shows the appearance or disappearance of chemical groups after curing of the resins [24]. Thermal analysis of resins with differential scanning calorimetry and thermogravimetric analysis monitors the thermal stability of the resins and the pure tannins and lignins that give the maximum temperature at which they can be used and an insight into the major chemical structures of the compounds [7, 24, 31].

This study aims to prepare tannin–lignin adhesives from mimosa tannins and glyoxalated ammonium lignosulfonates and sodium lignosulfonates. For the first time, two ammonium lignosulfonates and two sodium lignosulfonates were glyoxalated, and their thermal stability was studied before and after treatment by thermogravimetric analysis and differential scanning calorimetry. These lignosulfonates were used to make tannin–lignin adhesives with different proportions of tannins and lignosulfonates and with the different lignosulfonates. The thermal properties of these adhesives were evaluated by thermogravimetric analysis, differential scanning calorimetry and thermomechanical analysis.

## Materials and methods

### Material

Lignins used in this work were two different sodium lignosulfonates (NaLSP and NaLSL) types and two different ammonium lignosulfonates (NH4LSL and NH4LSP) types delivered by Tembec (Tartas, France). The mimosa tannin extracts were provided by Silvateam (Italy). The sodium hydroxide, hexamethylenetetramine (hexamine) and the glyoxal (40 %) were purchased from Fisher Scientific (Waltham, USA).

### Glyoxalation of lignosulfonates

The glyoxalation of the four lignosulfonates was carried out as described by El Mansouri [10]. 29.5 parts by mass of dry lignin were slowly added to 38.4 parts of water. Sodium hydroxide solution (33 %) was added in order to keep the pH of the solution between 12 and 12.5 for better dissolution of the lignin. A 800-mL flat-bottom flask equipped with a condenser, and a magnetic stirrer bar was charged with the above solution and heated to 58 °C. 17.5

**Table 1** Lignosulfonates characteristics

Identification	Type	Aspect	pH
NaLSP	Sodium lignosulfonate	Brown powder	8.5
NaLSL	Sodium lignosulfonate	Dark liquid	8.3
NH4LSL	Ammonium lignosulfonate	Dark liquid	3.6
NH4LSP	Ammonium lignosulfonate	Brown powder	5.6

**Table 2** Adhesive formulations

Formulations	Tannins/ mass%	Glyoxalated lignins/mass%	pH
Mimosa– NaLSP	20	80	9.08
	40	60	10.10
	50	50	9.84
	60	40	10.33
NaLSL	40	60	10.10
NH4LSL	40	60	9.97
NH4LSP	40	60	10.05

parts by mass glyoxal (40 % in water) were added, and the lignin solution was then continuously stirred with a magnetic stirrer/hot plate for 8 h. The solid contents for all glyoxalated lignin were around 43 %. The lignosulfonates characteristics are presented in Table 1.

### Adhesive formulation

A 45 % mimosa tannin solution in water was prepared. A sodium hydroxide solution (33 %) was added in order to keep the pH of the solution at 10.4. The pH was chosen for the hardener performs at its best at that pH, and tannins dissolve at high pH; 5 % of a hexamethylenetetramine (hexamine) (solid mass of hexamine on solid mass of tannins) was added as hardener. The hexamine was added as a solution at a concentration of 30 % in water.

In this paper, we studied four different ratios of tannin–glyoxalated lignin adhesive formulations for the sodium lignosulfonate NaLSP. Mimosa tannin–glyoxalated lignin adhesive formulations were also produced with other lignosulfonates for one ratio. Different formulations are described in Table 2.

### Thermomechanical analysis (TMA)

The curing kinetics and mechanical properties of the adhesives were measured by TMA by monitoring the rigidity of a bonded wood joint as a function of temperature. The analyses were performed on a Mettler Toledo

TMA SDTA 840. 30 mg of resin was placed between two plies of maritime pine wood to form a joint of  $17 \times 5 \times 1.2$  mm. The bonded wood joints were submitted to three points bending on a span of 14 mm and subjected to an alternating force of 0.1/0.5 N with a 6 s/6 s cycle. The heating rate was of  $10 \text{ }^\circ\text{C min}^{-1}$  from 25 to  $250 \text{ }^\circ\text{C}$ . For each formulation, five replicates were done. The results were analysed using STARE software.

#### Thermogravimetric analysis (TG)

The thermal stability of the cured resins and of the raw materials was determined by thermogravimetric analysis, TA Instrument TGA Q500. The samples were made of cured resin and analysed from 30 to  $600 \text{ }^\circ\text{C}$  at a heating rate of  $10 \text{ }^\circ\text{C min}^{-1}$  under  $40\text{--}60 \text{ mL min}^{-1} \text{ N}_2$ . The results were analysed with Universal Analysis software.

#### Differential scanning calorimetry (DSC)

DSC data were obtained with a TA Instrument DSC Q20. The samples were made of 5–8 mg of cured resin and of glyoxalated and non-glyoxalated lignosulfonates and were put in an aluminium crucible. The temperature scanned from 30 to  $250 \text{ }^\circ\text{C}$  at heating rate of  $10 \text{ }^\circ\text{C min}^{-1}$  under  $50 \text{ mL min}^{-1} \text{ N}_2$ . The results were analysed with Universal Analysis software.

#### Fourier transformed infrared (FTIR)

FTIR spectra were recorded on a Perkin Elmer Spectrum One equipped with an ATR-FTIR unit. A few milligrams of ground extract sample were placed on a crystal (diamond/ZnSe). The spectra were obtained with a resolution of  $4 \text{ cm}^{-1}$  and four co-addition scans in a wavelength range of  $650\text{--}4,000 \text{ cm}^{-1}$ . The spectra were collected and analysed using Spectrum software (Perkin Elmer).

#### Statistical analysis

The data are presented as mean  $\pm$  SD values. The TMA values were analysed with the Bartlett test, Tukey's HSD test and the ANOVA test. All the statistical analyses were carried out at  $p < 0.05$  significance level.

## Results and discussion

#### Analysis of lignosulfonates before and after glyoxalation

The thermal decomposition of the lignosulfonates before and after glyoxalation was determined by TG. The TG

curve presents the mass loss of the lignosulfonates in relation to the temperature, and the first derivative of that curve (DTG) shows the corresponding rate of mass loss. The TG curves and DTG curves for the lignosulfonates NaLSP and NH4LSP are presented in Fig. 1. NaLSP and NaLSL present similar curves, and NH4LSL and NH4LSP also present similar curves.

In a first step, which occurs up to approximately  $110 \text{ }^\circ\text{C}$ , the mass loss is due to the elimination of any residual water. In a second step, the non-glyoxalated ammonium lignosulfonates start to decompose at  $171\text{--}176 \text{ }^\circ\text{C}$ . The non-glyoxalated sodium lignosulfonates start to decompose at  $186\text{--}202 \text{ }^\circ\text{C}$ . The decomposition occurs up to

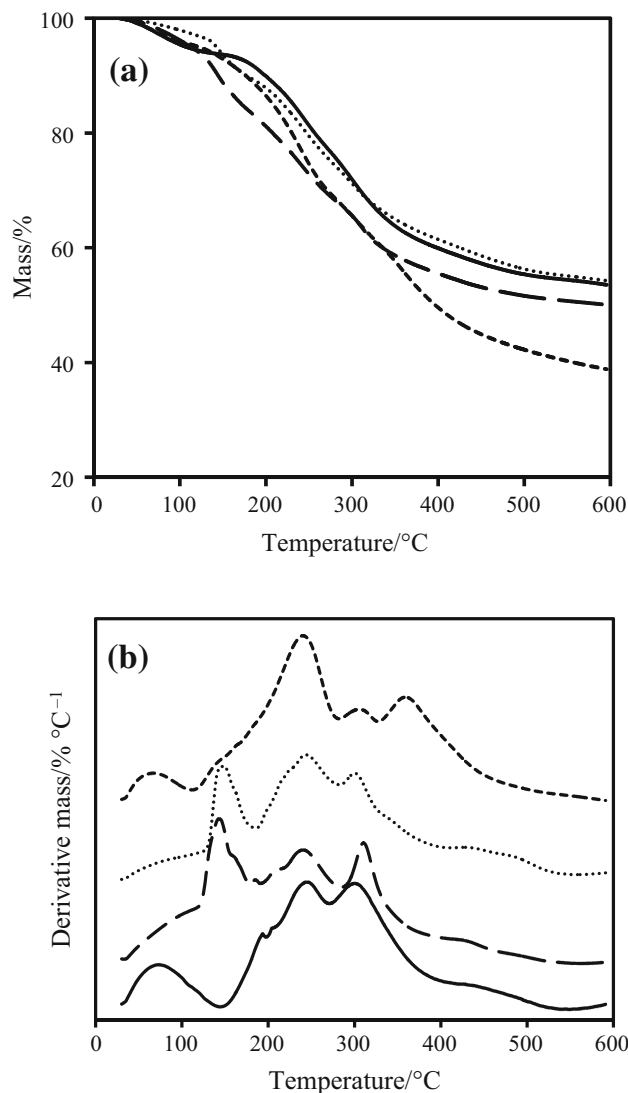


**Fig. 1** a TG curves and b DTG curves of (continuous solid line) non-glyoxalated NaLSP; (continuous spaced solid line) glyoxalated NaLSP; (continuous dashed line) non-glyoxalated NH4LSP and (continuous dotted line) glyoxalated NH4LSP recorded at  $10 \text{ }^\circ\text{C min}^{-1}$

375–400 °C with a mass loss of 30–40 %, except for NaLSL which undergoes degradation up to 345 °C and 23 % mass loss. The glyoxalated lignosulfonates are less stable to temperature, and the second step started at 125–135 °C and terminated at 330–345 °C. This early mass loss is caused by the link formed by the glyoxal that is less stable. This might be due to the low reactivity of glyoxal, which introduces much earlier sites of tridimensional cross-linking in the network. The network is weaker, and degradation starts at lower temperatures. Another hypothesis is that there is formation of glyoxal-*O*-glyoxal unstable bridges that on heating should rearrange to a simple glyoxal bridge, as formaldehyde does. However, due to the low reactivity of glyoxal, it is unable to rearrange to a single bridge causing instability. The mass loss of glyoxalated lignosulfonates during this second step is of 30–33 %. After heating to 600 °C, there is still up to 45–60 % of the samples mass that has not been volatilised. According to Tejado et al. [32], the mass loss occurring after 500 °C is due to the decomposition of aromatic rings.

The DTG max appears at approximately 240–245 °C for all the lignosulfonates and glyoxalated lignosulfonates (Fig. 1b). Khan et al. [6] attributed this mass loss to a breakdown of side chains present in lignin. Non-glyoxalated sodium lignosulfonates present a DTG peak at 300 °C, and the non-glyoxalated ammonium lignosulfonates present a DTG peak at 360 °C. After glyoxalation, the ammonium lignosulfonates show a DTG peak at 300 °C whereas the sodium lignosulfonates at 310 °C. Between 300 and 450 °C, a pyrolytic degradation occurs which leads to the fragmentation of the intermolecular bonding and the release of monomeric phenols [4, 32]. After glyoxalation, a mass loss appears between 130 and 170 °C with a peak at 145 °C. This mass loss does not appear with alkaline rice straw lignin [31].

DSC analyses were also performed on all lignosulfonates (Fig. 2). Prior to the analysis, the lignosulfonates were dried at 60 °C until the mass had stabilised. The non-glyoxalated lignosulfonates are stable to temperature. An endothermic transition occurs at 136 °C for glyoxalated sodium lignosulfonates. The glyoxalated ammonium lignosulfonates show an endotherm at 145–149 °C. These transitions correspond to the glass transition of the lignosulfonates and are found in the same range of temperature as kraft lignins or organosolv lignins [4, 32]. The endotherms that take place at 190–200 °C and at 210–235 °C are present for all the glyoxalated lignosulfonates and are higher for glyoxalated NaLSL. They correspond to the degradation of the lignosulfonates.

All the lignosulfonates, before and after glyoxalation, were studied by FTIR in the range of 650–2,000  $\text{cm}^{-1}$  region (Fig. 3). The analyses of the spectra are based on the assignments given by Boeriu and Bravo [33]. The two

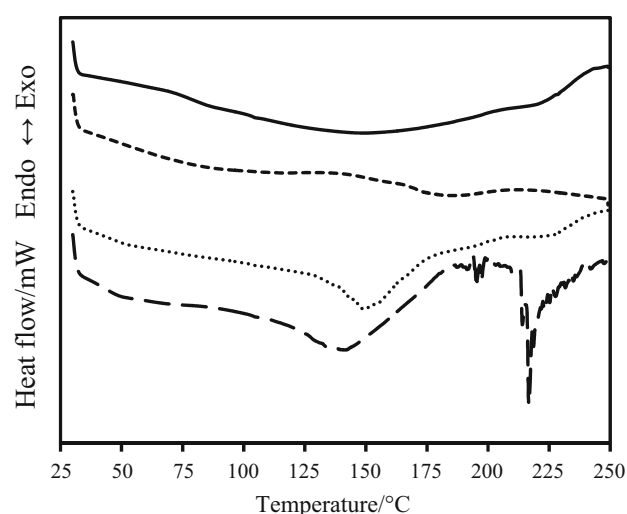


**Fig. 2** DSC curves of (continuous solid line) non-glyoxalated NaLSL; (continuous spaced solid line) glyoxalated NaLSL; (continuous dashed line) non-glyoxalated NH4LSL and (continuous dotted line) glyoxalated NH4LSL recorded at  $10\text{ }^{\circ}\text{C min}^{-1}$

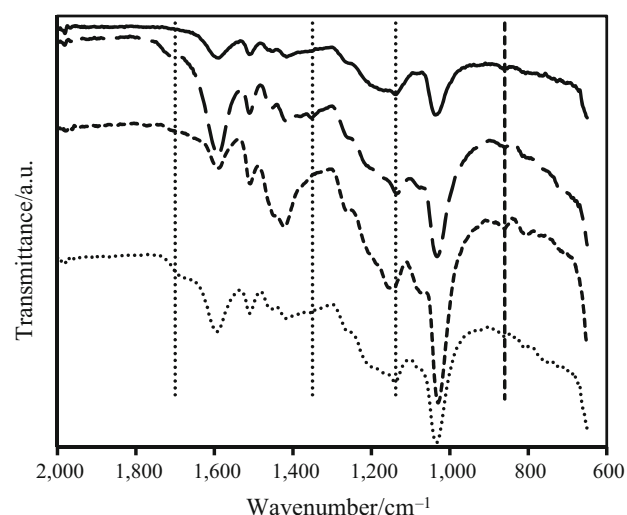


**Fig. 3** FTIR spectra of (continuous solid line) non-glyoxalated NaLSL; (continuous spaced solid line) glyoxalated NaLSL; (continuous dashed line) non-glyoxalated NH4LSP and (continuous dotted line) glyoxalated NH4LSP

ammonium lignosulfonates were identical as were the two sodium lignosulfonates. When comparing two ammonium lignosulfonates and two sodium lignosulfonates before treatment, we can see small differences between the two types of lignosulfonates. The ammonium lignosulfonates show bands at 1,075, 860 and 808  $\text{cm}^{-1}$  that are not present in sodium lignosulfonates. These bands correspond to carbohydrate vibration, C–H out of plane vibrations from guaiacyl units and other aromatic C–H stretch vibrations, respectively. After glyoxalation, when comparing ammonium lignosulfonates to sodium lignosulfonates, the FTIR

spectra are similar. The only differences can be found in the range of 1,680–1,715  $\text{cm}^{-1}$  region. Glyoxalated ammonium lignosulfonates have a band at 1,680  $\text{cm}^{-1}$ , and glyoxalated sodium lignosulfonates present a band at 1,715  $\text{cm}^{-1}$  which are assigned to conjugated carbonyl/carboxyl stretching. After glyoxalation, ammonium lignosulfonates show a shift of the band at 1,155–1,140  $\text{cm}^{-1}$  which is assigned to C–O stretch vibration. Peaks at 1,715–1,680, 1,350 and 1,140  $\text{cm}^{-1}$  are present only after glyoxalation and are attributed to carbonyl/carboxyl stretching, phenolic hydroxyl groups and C–O stretch vibration, respectively.

Analysis of the resin’s curing

The three bending-point modes enabled us to get the deflection curves from which the modulus of elasticity (MOE) of the resins is determined. The MOE is a good indicator of the adhesive behaviour during curing and its wood-joint strength.

The influence of four proportions of tannins–glyoxalated lignosulfonates on the adhesive properties is studied. The curves of MOE as a function of temperature are given in Fig. 4. The tannin proportions varied from 20, 40, 50 and 60 mass%. All the adhesives show an increase of the MOE at 100–110 °C. According to Ping et al. [34], this corresponds to a first cross-linking reaction through formation of a non-stable cross-linker. The highest MOE values are obtained at 160–170 °C. There is a decrease in the MOE at 170–190 °C that corresponds to the degradation of wood components and

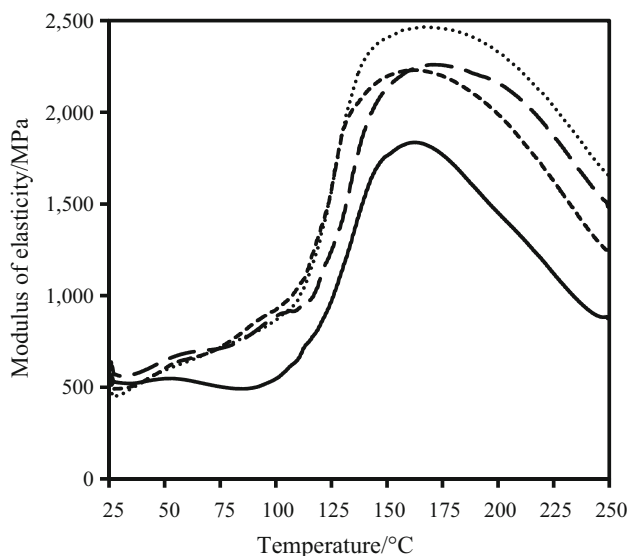


**Fig. 4** Module of elasticity of average curves of a pine joint as a function of temperature obtained by TMA testing when bonded with mimosa tannins–glyoxalated NaLSP-cured resins\*\*\*: (continuous solid line) 20 mass% tannins; (continuous spaced solid line) 40 mass% tannins; (continuous dashed line) 50 mass% tannins; (continuous dotted line) 60 mass% tannins recorded at 10 °C min<sup>-1</sup>

of the adhesive. A comparison of the TMA profiles shows that the less the tannins added, the lower the MOE. The maximum values of MOE are presented in Table 3. There are statistically no significant differences between the MOE of the adhesive formulations containing 40, 50 and 60 mass% of mimosa tannins (Tukey HSD test,  $p$  value = 0.997,  $p$  value = 0.379,  $p$  value = 0.493). The adhesive formulation with 20 mass% of mimosa tannins is not statistically different than the formulations with 40 and 50 mass% mimosa tannins (Tukey HSD test,  $p$  value = 0.091 and  $p$  value = 0.061). However, the MOE of the adhesive formulation containing 20 mass% of mimosa tannins is statistically lower than the adhesive with 60 mass% of mimosa tannins (Tukey HSD test,  $p$  value = 0.003).

As lignosulfonates are co-products in pulp mills and there are no significant differences between adhesive formulations with 40 mass% tannins and 60 mass% tannins, it was decided that adhesives with NaLSL, NH4LSL and NH4LSP lignosulfonates would have 40 mass% mimosa tannins and 60 mass% of glyoxalated lignosulfonates. The curves of MOE as a function of temperature, obtained by TMA for resins with the different lignosulfonates, are given in Fig. 5. All curves increase at 110 °C, which corresponds to a first cross-linking reaction through formation of a non-stable cross-linker. The maximum MOE values are obtained between 160 and 180 °C. The maximum values of MOE are presented in Table 3. There are statistically no significant differences between the MOE of the adhesive formulations with 40 mass% mimosa tannins and 60 mass% NaLSP, 60 mass% NaLSL, 60 mass% NH4LSL and 60 mass% NH4LSP (Anova test,  $p$  value = 0.457). The wood joint bonded with the adhesive formulation with NaLSL has a slightly higher MOE between 137 and 208 °C compared to the adhesive formulations with NaLSP, NH4LSL and NH4LSP. The adhesive formulations with

**Table 3** Module of elasticity values for all the adhesive formulations

Formulation	Maximum MOE/MPa*	Temperature/°C
Mimosa–NaLSP (20–80)	1,905 ± 99 <sup>ac</sup>	159
Mimosa–NaLSP (40–60)	2,264 ± 110 <sup>abcd</sup>	168
Mimosa–NaLSP (50–50)	2,294 ± 308 <sup>abc</sup>	157
Mimosa–NaLSP (60–40)	2,497 ± 285 <sup>bc</sup>	165
Mimosa–NaLSL (40–60)	2,483 ± 394 <sup>bd</sup>	165
Mimosa–NH4LSL (40–60)	2,325 ± 260 <sup>bd</sup>	165
Mimosa–NH4LSP (40–60)	2,185 ± 65 <sup>bd</sup>	176

\* Standard deviation of five replicates

<sup>a,b</sup> Group of values with significant differences between each group

<sup>c</sup> The means were analysed with Tukey’s HSD test at  $p < 0.05$

<sup>d</sup> The means were analysed with the Anova test at  $p < 0.05$ ,  $p$  value = 0.457

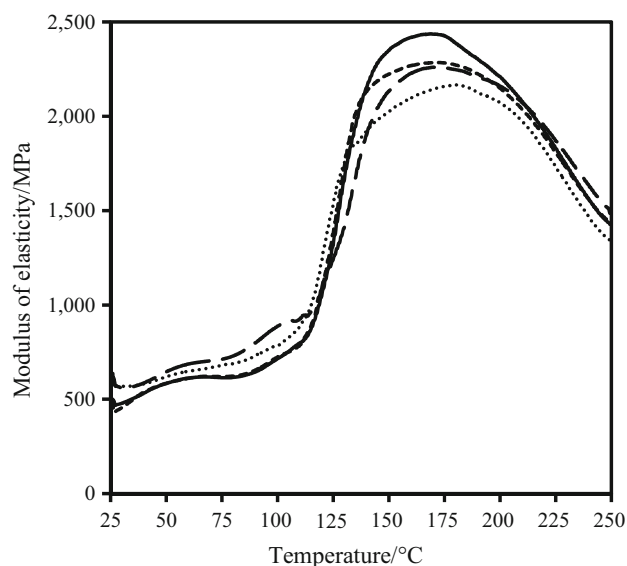


**Fig. 5** Module of elasticity of average curves of a pine joint as a function of temperature obtained by TMA testing when bonded with (continuous solid line) mimosa tannins–glyoxalated NaLSP; (continuous spaced solid line) mimosa tannins–glyoxalated NaLSP; (continuous dashed line) mimosa tannins–glyoxalated NH4LSL; (continuous dotted line) mimosa tannins–glyoxalated NH4LSP recorded at  $10\text{ }^{\circ}\text{C min}^{-1}$

NaLSP and NH4LSL have a higher MOE between 135 and 250 °C compared to the adhesive with NH4LSP. The adhesive formulation with NaLSP shows a slower cross-linking reaction than the adhesives with NaLSL, NH4LSL and NH4LSP. Similar results have been found for mimosa tannins–glyoxalated organosolv lignin–pMDI (polymeric 4,4'-diphenyl methane diisocyanate) adhesives [16]. Navarrete et al. [21] found similar results for mimosa tannins–glyoxalated organosolv lignins using hexamine as a hardener for a tannin–lignin ratio of 50–50; however, resins with a 60–40 ratio presented higher MOE.

#### Thermal analysis of cured resins

The TG curves of the cured resins with glyoxalated NaLSP in different proportions are presented in Fig. 6. The initial decomposition temperature and the final decomposition temperature of the resins were observed. In a first stage, the resins are submitted to the elimination of water, in which 8–15 % of mass loss occurs depending on the initial water content of the samples. In a second stage, the resin with 20 mass% mimosa tannins starts to decompose at 238 °C, the one with 40 mass% starts its degradation at 242 °C, the cured resin with 50 mass% tannins at 258 °C and the adhesive with 60 mass% tannins decomposes at 222 °C. When the proportion of tannins increases, the initial decomposition starts at higher temperatures up to 50 mass% of tannins after which the decomposition starts at lower temperatures. This decomposition could be the

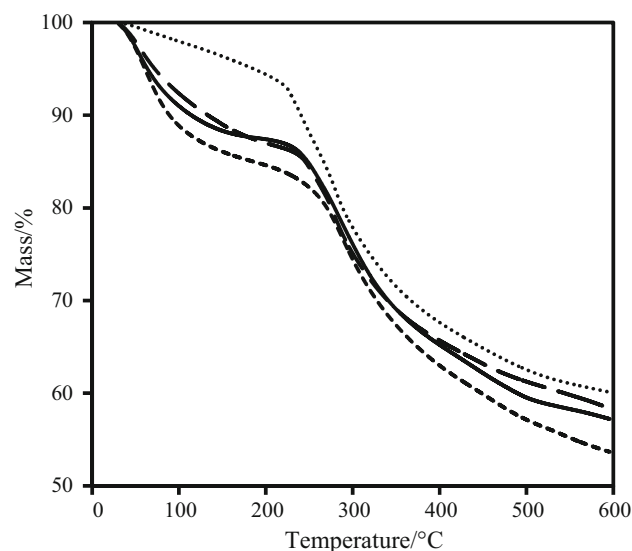


**Fig. 6** TG curves of mimosa tannins–glyoxalated NaLSP cured resins: (continuous solid line) 20 mass% tannins; (continuous spaced solid line) 40 mass% tannins; (continuous dashed line) 50 mass% tannins; (continuous dotted line) 60 mass% tannins recorded at  $10\text{ }^{\circ}\text{C min}^{-1}$

result of a partial breakdown of the intermolecular bonding [24] and occurs up to approximately 377–392 °C. The mass loss progressively increases with the temperature up to 600 °C where the mass loss starts to stabilise. The mass loss ranges from 30 to 36 %. Similar mass losses were found for mimosa tannin resins [24].

The TG curves of the cured resins with 40 mass% mimosa tannins with four glyoxalated lignosulfonates are presented in Fig. 7. The initial decomposition temperature and the final decomposition temperature of the resins were observed. In the first stage, the resins are submitted to the elimination of water, in which 3–12 % mass loss occurs depending on the initial water content of the samples. In the second stage, the resin with NaLSL starts to decompose at 191 °C, the one with NaLSP starts its degradation at 242 °C, the cured resin with NH4LSL at 197 °C and the adhesive with NH4LSP decomposes at 201 °C. The resin with NaLSP is the most stable to temperature. This decomposition could be the result of a partial breakdown of the intermolecular bonding and occurs up to approximately 369–379 °C. The mass loss progressively increases with the temperature up to 600 °C where the mass loss starts to stabilise. The mass loss ranges from 31 to 41 %. Similar mass losses were found for mimosa tannin resins and valonia tannin resins [24].

The DTG curves of mimosa tannins, glyoxalated NH4LSL and of the adhesive formulation with NH4LSP are presented in Fig. 8. Four major mass losses are present for mimosa tannins. The first one, at 56 °C, corresponds to

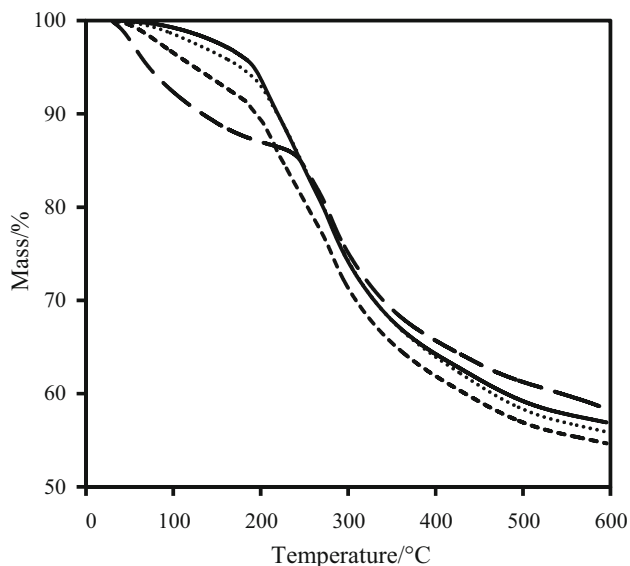


**Fig. 7** TG curves of mimosa tannins–glyoxalated lignosulfonates with 40 mass% tannins cured resins: (*continuous solid line*) mimosa tannins–glyoxalated NaLSL; (*continuous spaced solid line*) mimosa tannins–glyoxalated NaLSP; (*continuous dashed line*) mimosa tannins–glyoxalated NH4LSL; (*continuous dotted line*) mimosa tannins–glyoxalated NH4LSP recorded at  $10\text{ }^{\circ}\text{C min}^{-1}$

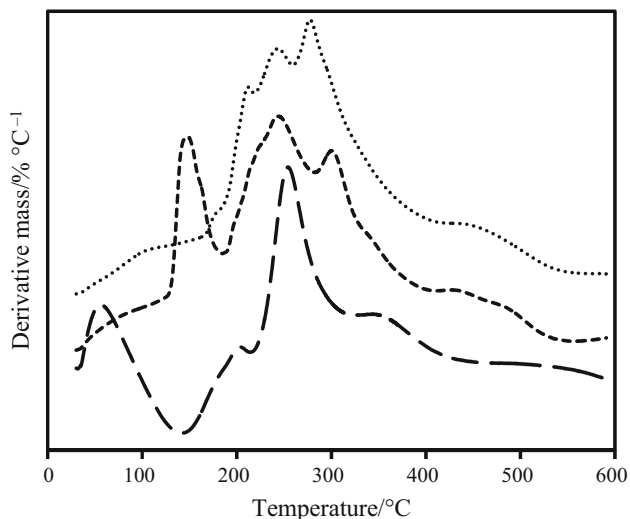


**Fig. 8** DTG curves of (*continuous spaced solid line*) mimosa tannins; (*continuous dotted line*) glyoxalated NH4LSP and (*continuous dashed line*) mimosa tannins–glyoxalated NH4LSP recorded at  $10\text{ }^{\circ}\text{C min}^{-1}$

the elimination of water. At  $200\text{ }^{\circ}\text{C}$ , the mass loss corresponds to the degradation of hydroxyl, ether and ester groups [35]. The mass loss at  $253\text{ }^{\circ}\text{C}$  is due to decarboxylation of the mimosa tannins. At  $355\text{ }^{\circ}\text{C}$ , the mass loss corresponds to further degradation of hydroxyl groups [36]. The mimosa tannins and the cured resins have no common peaks, and the mimosa has completely reacted during the curing process. The DTG curve of the cured resin has

several peaks which correspond to the degradation of the lignosulfonates that did not react during the curing process, at  $243\text{ }^{\circ}\text{C}$ , and from approximately  $335\text{--}600\text{ }^{\circ}\text{C}$ . The cured resin shows a DTG peak at  $243\text{ }^{\circ}\text{C}$ , which corresponds to a breakdown of side chains present in the remaining lignosulfonates. The disappearance of the degradation peaks in the cured resin at  $147\text{ }^{\circ}\text{C}$  and at  $300\text{ }^{\circ}\text{C}$  which correspond to the glass transition NH4LSP and to inter-unit degradation of the glyoxalated lignosulfonate NH4LSP, respectively, confirm that most of the glyoxalated NH4LSP has reacted.

The DSC results for cured resins with 40 mass% mimosa tannins are presented in Fig. 9. The adhesive formulation with NaLSP 40 mass% mimosa tannins is stable up to  $233\text{ }^{\circ}\text{C}$ , the resin with NaLSL is stable until  $198\text{ }^{\circ}\text{C}$ , the resin with NH4LSL is stable until  $216\text{ }^{\circ}\text{C}$ , where an endothermic reaction takes place. This reaction is a consequence of the degradation of the resins. The DSC and TG results both show that all the resins are stable to temperature up to at least  $190\text{ }^{\circ}\text{C}$ . The resins with the sodium lignosulfonate NaLSP are more stable and are not submitted to a thermal degradation until  $222\text{ }^{\circ}\text{C}$ .

In order to understand the chemical reactions that take place during the curing of the resins, FTIR analyses were carried out, and the spectra of the mimosa tannins–glyoxalated NaLSL, mimosa tannins, glyoxalated NaLSL and hexamine are presented in Fig. 10. When comparing the cured adhesive to the raw materials used, we can notice that the hardener (hexamine) has totally reacted. The cured

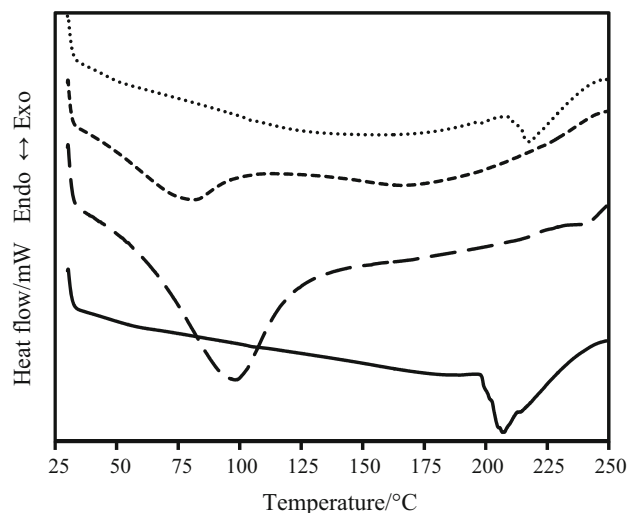


**Fig. 9** DSC curves of mimosa tannins–glyoxalated lignosulfonates with 40 mass% tannins cured resins: (*continuous solid line*) mimosa tannins–glyoxalated NaLSL; (*continuous spaced solid line*) mimosa tannins–glyoxalated NaLSP; (*continuous dashed line*) mimosa tannins–glyoxalated NH4LSL; (*continuous dotted line*) mimosa tannins–glyoxalated NH4LSP recorded at  $10\text{ }^{\circ}\text{C min}^{-1}$

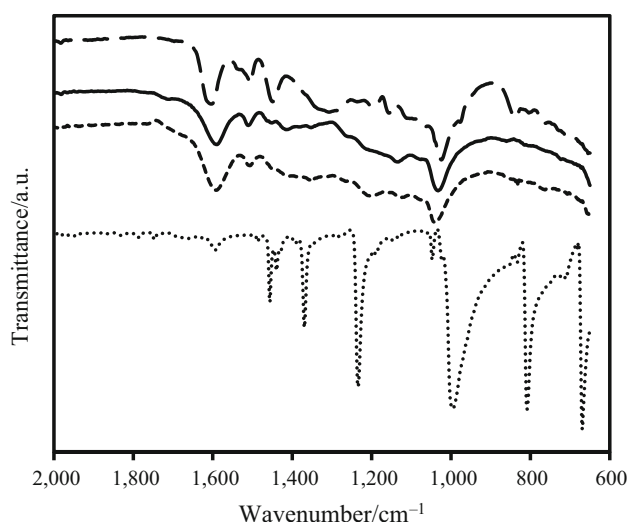


**Fig. 10** FTIR spectra of (*continuous spaced solid line*) mimosa tannins; (*continuous solid line*) glyoxalated NaLSL; (*continuous dashed line*) mimosa tannins–glyoxalated NaLSL and (*continuous dotted line*) hexamine

resin spectrum is very similar to the glyoxalated NaLSL spectrum. The only bands not shared are at 1,740 and 1,715  $\text{cm}^{-1}$ , which are assigned to carbonyl/carboxyl groups and at 840–835  $\text{cm}^{-1}$  and at 765  $\text{cm}^{-1}$ , which correspond to aromatic C–H “oop” stretch, respectively. The carbonyl/carboxyl groups from the glyoxalated lignosulfonates react during curing and disappear in the resin. The cured resin and the mimosa tannins spectra only have a few bands in common that are not present in the glyoxalated NaLSL at 840–835  $\text{cm}^{-1}$  and at 765  $\text{cm}^{-1}$ .

Autocondensation of mimosa tannins occurs at high alkalinity, pH 10 or higher [35]. At lower pH, mimosa tannins cross-link with hexamine. As our adhesive solutions are at approximately pH 10, mimosa tannins are subjected to both autocondensation reactions and cross-linking reactions with hexamine and the glyoxalated lignosulfonates.

## Conclusions

In this study, we monitored the thermal stability of sodium and ammonium lignosulfonates before and after glyoxalation. After glyoxalation, the lignosulfonates have a glass transition at 136 °C for sodium lignosulfonates and at 145–149 °C for ammonium lignosulfonates. The glyoxalation reaction lessens the thermal durability of all lignosulfonates.

We assessed the optimum proportion of mimosa tannins–glyoxalated NaLSP. The resins with 40, 50 and 60 mass% mimosa tannins are statistically the same and give more efficient adhesives than the adhesive formulation with 20 mass% mimosa tannins. The adhesive formulations with

sodium lignosulfonates or ammonium lignosulfonates gave the same maximum of modulus of elasticity.

The cured resins with glyoxalated NaLSL, NH<sub>4</sub>LSL and NH<sub>4</sub>LSP are stable up to 190–200 °C. The adhesive formulations with NaLSP are more thermally stable than the ones with the other lignosulfonates. They are stable up to 222–258 °C. Further analysis by TG-MS or TG-FTIR would give more information on the chemical structures of the cured resins.

**Acknowledgements** We gratefully acknowledge the financial support of the “Conseil Général des Landes” and of ANR-10-EQPX-16 Xyloforest. We also thank Tembec Company (Tartas 40 - France) for providing lignosulfonate samples.

## References

- Sellers T. Wood adhesive innovations and applications in North America. *For Prod J.* 2001;51:12–22.
- Gomez-Bueso J, Haupt R. Chapter 8: wood composite adhesives. In: Pilato L, editor. *Phenolic resins a century progress*. Berlin, Heidelberg: Springer Berlin Heidelberg; 2010. p. 155–87.
- Cheng S, Yuan Z, Leitch M, Anderson M, Xu C. Highly efficient de-polymerization of organosolv lignin using a catalytic hydro-thermal process and production of phenolic resins/adhesives with the depolymerized lignin as a substitute for phenol at a high substitution ratio. *Ind Crop Prod.* 2013;44:315–22.
- El Mansouri N-E, Yuan Q, Huang F. Characterization of alkaline lignins for use in phenol-formaldehyde and epoxy resins. *Bio-Resources.* 2011;6:2647–62.
- Khan MA, Ashraf SM, Malhotra VP. Development and characterization of a wood adhesive using bagasse lignin. *Int J Adhes Adhes.* 2004;24:485–93.
- Khan MA, Ashraf SM, Malhotra VP. Eucalyptus bark lignin substituted phenol formaldehyde adhesives: a study on optimization of reaction parameters and characterization. *J Appl Polym Sci.* 2004;92:3514–23.
- Khan MA, Ashraf SM. Studies on thermal characterization of lignin: substituted phenol formaldehyde resin as wood adhesives. *J Therm Anal Calorim.* 2007;89:993–1000.
- Matuana LM, Riedl B, Barry AO. Caractérisation cinétique par analyse enthalpique différentielle des résines phenol-formaldehyde à base de lignosulfonates. *Eur Polym J.* 1993;29:483–90.
- Moubarik A, Grimi N, Boussetta N, Pizzi A. Isolation and characterization of lignin from Moroccan sugar cane bagasse: production of lignin–phenol-formaldehyde wood adhesive. *Ind Crop Prod.* 2013;45:296–302.
- El Mansouri N, Pizzi A, Salvadó J. Lignin-based wood panel adhesives without formaldehyde. *Holz als Roh- und Werkst.* 2007;65:65–70.
- El Mansouri N-E, Pizzi A, Salvadó J. Lignin-based polycondensation resins for wood adhesives. *J Appl Polym Sci.* 2007;103:1690–9.
- Kielhorn J, Pohlenz-Michel C, Schmidt S, Mangelsdorf I. Glyoxal (concise international chemical assessment document 57) World Health Organization. 2004
- Navarrete P, Mansouri HR, Pizzi A, Tapin-Lingua S, Benjelloun-Mlayah B, Pasch H, et al. Wood panel adhesives from low molecular mass lignin and tannin without synthetic resins. *J Adhes Sci Technol.* 2010;24:1597–610.



14. Ballerini A, Despres A, Pizzi A. Non-toxic, zero emission tannin-glyoxal adhesives for wood panels. *Holz als Roh- und Werkst.* 2005;63:477–8.
15. El Mansouri N-E, Yuan Q, Huang F. Synthesis and characterization of kraft lignin-based epoxy resins. *BioResources.* 2011;6:2492–503.
16. Lei H, Pizzi A, Du G. Environmentally friendly mixed tannin/lignin wood resins. *J Appl Polym Sci.* 2008;107:203–9.
17. Ping L, Pizzi A, Guo ZD, Brosse N. Condensed tannins from grape pomace: characterization by FTIR and MALDI TOF and production of environment friendly wood adhesive. *Ind Crop Prod.* 2012;40:13–20.
18. Vázquez G, González-Alvarez J, Santos J, Freire MS, Antorrena G. Evaluation of potential applications for chestnut (*Castanea sativa*) shell and eucalyptus (*Eucalyptus globulus*) bark extracts. *Ind Crop Prod.* 2009;29:364–70.
19. Gornik D, Hemingway RW, Tisler V. Tannin-based cold-setting adhesives for face lamination of wood. *Holz als Roh- und Werkst.* 2000;58:23–30.
20. Kim S. Environment-friendly adhesives for surface bonding of wood-based flooring using natural tannin to reduce formaldehyde and TVOC emission. *Bioresour Technol.* 2009;100:744–8.
21. Navarrete P, Pizzi A, Tapin-Lingua S, Benjelloun-Mlayah B, Pasch H, Rode K, et al. Low formaldehyde emitting biobased wood adhesives manufactured from mixtures of tannin and glyoxylated lignin. *J Adhes Sci Technol.* 2012;26:1667–84.
22. Jorge FC, Pascoal Neto C, Irle MA, Gil MH, Pedrosa de Jesus J. Wood adhesives derived from alkaline extracts of maritime pine bark: preparation, physical characteristics and bonding efficacy. *Holz als Roh- und Werkst.* 2002;60:303–10.
23. Lu Y, Shi Q, Gao Z. Thermal analysis and application of larch tannin-based adhesive for plywood and hardboard. *Holz als Roh- und Werkst.* 1995;53:205–8.
24. Özacar M, Soykan C, ŞengiL İA. Studies on synthesis, characterization, and metal adsorption of mimosa and valonia tannin resins. *J Appl Polym Sci.* 2006;102:786–97.
25. Vázquez G, González-Alvarez J, Lopez-Suevos F, Freire S, Antorrena G. Curing kinetics of tannin–phenol-formaldehyde adhesives as determined by DSC. *J Therm Anal Calorim.* 2002;70:19–28.
26. Vázquez G, González-Alvarez J, Antorrena G. Curing of a phenol-formaldehyde–tannin adhesive in the presence of wood: analysis by differential scanning calorimetry. *J Therm Anal Calorim.* 2006;84:651–4.
27. Pichelin F, Kamoun C, Pizzi A. Hexamine hardener behaviour: effects on wood glueing, tannin and other wood adhesives. *Holz als Roh- und Werkst.* 1999;57:305–17.
28. Moubarik A, Mansouri HR, Pizzi A, Charrier F, Allal A, Charrier B. Corn flour-mimosa tannin-based adhesives without formaldehyde for interior particleboard production. *Wood Sci Technol.* 2013;47:675–83.
29. Pichelin F, Nakatani M, Pizzi A, Wieland S, Despres A, Rigolet S. Structural beams from thick wood panels bonded industrially with formaldehyde-free tannin adhesives. *For Prod J.* 2006;56:31–6.
30. El Hage R, Brosse N, Navarrete P, Pizzi A. Extraction, characterisation and utilization of organosolv *Miscanthus* lignin for the conception of resin for wood adhesives. *J Adhes Sci Technol.* 2011;25:1549–60.
31. El Mansouri N-E, Yuan Q, Huang F. Study of chemical modification of alkaline lignin by the glyoxalation reaction. *BioResources.* 2011;6:4523–36.
32. Tejado A, Peña C, Labidi J, Echeverria JM, Mondragon I. Physico-chemical characterization of lignins from different sources for use in phenol-formaldehyde resin synthesis. *Bioresour Technol.* 2007;98:1655–63.
33. Boeriu CG, Bravo D, Gosselink RJA, van Dam JEG. Characterisation of structure-dependent functional properties of lignin with infrared spectroscopy. *Ind Crop Prod.* 2004;20:205–18.
34. Ping L, Brosse N, Chrusciel L, Navarrete P, Pizzi A. Extraction of condensed tannins from grape pomace for use as wood adhesives. *Ind Crop Prod.* 2011;33:253–7.
35. Peña C, de la Caba K, Retegi A, Ocando C, Labidi J, Echeverria JM, et al. Mimosa and chestnut tannin extracts reacted with hexamine in solution. *J Therm Anal Calorim.* 2009;96:515–21.
36. Garro Galvez JM, Riedl B, Conner AH. Analytical studies on tara tannins. *Holzforschung.* 1997;51:235–43.